Key Engineering Materials
ISSN: 1662-9795, Vol. 926, pp 612-620
doi:10.4028/p-aynwq8

Submitted: 2021-12-09
Revised: 2022-01-26
Accepted: 2022-01-26
Online: 2022-07-22

Impact of a Splined Mandrel Geometry on Die Filling in a Cold Forging Process with Adjustable Deformation Zone

Alexander Weiß[1,a *], Mario Arny[1,b] and Mathias Liewald[1,c]

[1]University of Stuttgart, Institute for Metal Forming Technology (IFU),

Holzgartenstraße 17, 70174 Stuttgart, Germany

[a]alexander.weiss@ifu.uni-stuttgart.de, [b]st143731@stud.uni-stuttgart.de,
[c]mathias.liewald@ifu.uni-stuttgart.de

*corresponding author

Keywords: Cold forging, hollow shafts, internal splines

Abstract. Manufacturing of hollow components with local functional internal surfaces often requires complex process routes with several individual operations. By using a special hollow cold forging process with an adjustable deformation zone it is possible to manufacture hollow shafts with varying wall thickness over its axial length parts just within a single stroke of the press. Combining this principle with a splined mandrel allows manufacturing of tailored hollow shafts with local internal splines. However, the impact of geometry of mandrel and other process parameters on the shape of the cold forged internal splines have not been investigated yet. Furthermore, an underfilling phenomenon can occur on the outer surface of shaft during specific process states. In this contribution, several mandrel geometries and their impact on the part shape and filling / underfilling phenomenon in the mentioned process are investigated. To determine those effects, a numerical investigation has been conducted. Besides the geometry of the splined mandrel, also other parameters such as die geometry and tool kinematics were considered. The numerically calculated workpiece geometries are compared to the ideal geometries using a deviation analysis.

Introduction

Until today, lightweight design remains as crucial design factor in many technological and engineering fields. Usage of tailored hollow shafts provides high weight savings without reducing the section modulus of such hollow components significantly [1]. Furthermore, the increasing variety of drivetrain designs results in a demand for more flexible and versatile manufacturing processes in cold forging, so also low batch quantities can be produced more economically. A potential field of application of such huge variety of small electric drive systems is found in the sector of Light Electric Vehicles, including e-bikes, e-scooters and similar vehicles [2].

For highly stressed shafts which are used in such electric drive systems, cold forging processes are well suited for manufacturing due to the strain hardening of the material and beneficially hardened workpiece surface c. But in terms of flexibility, non-incremental forming processes, e.g. conventional cold forging, do not offer any potential for economic manufacturing of low batch quantities. Incremental forming processes, on the other hand, often do have longer process cycle times compared to non-incremental forming processes. To overcome these shortcomings of non-incremental forming processes a novel cold forging process has been developed at the Institute for Metal Forming Technology (IFU) at the University of Stuttgart. The new process provides manufacturing of hollow shafts with varying cross sections within one single stroke by means of an adjustable deformation zone. The working principle of this new process is described in [3].

However, manufacturing processes with an adjustable deformation zone are not entirely new. In the extrusion blow molding process for example, the thickness of the parison can be adjusted by moving a mandrel with its conical outside shape relatively to a stationary surrounding mold and, thus, the wall thickness of the part can be altered [4]. Further approaches have been carried out in hot extrusion of aluminum profiles with variable wall thickness design [5,6]. With regard to the cold forging process presented in this contribution, previous studies addressed numerical investigations

for production of hollow shafts with variable wall thickness [3] as well as a tool concept for the required tool kinematics [7]. Within these studies an underfilling phenomenon occurred on the part outer side that can be influenced by different process parameters [3]. This effect strongly depends on the adjustable deformation zone and is also known from hot extrusion of aluminum alloys [5] as well as cold drawing of tubes [8]. In [3] an approach for reduction of this effect has been presented comprising a higher internal back pressure between workpiece and mandrel by using a moveable splined mandrel. Tooth tips of this splined mandrel provide continuous contact with the workpiece material during the process and, therefore, in fact prevent severe underfillings. Since the correlation between the spline geometry and the cavity filling respectively underfilling of local workpiece features is not known from the state of the art so far, a detailed numerical investigation was carried out within the scope of this paper.

Material and Methods

The numerical investigations were performed using the FEM-software DEFORM. The flow curves of the annealed test material AISI 5115 (16MnCrS5) were determined by use of a thermo-mechanical simulator Gleeble 3800c at three different strain rates (0.1 s^{-1}, 1 s^{-1}, 10 s^{-1}) as well as several different temperatures ranging from 20°C up to 300°C. Although the process is intended to be performed at room temperature, also higher temperatures were included in the determination of the required flow curves to numerically represent softening of the material as a result of a local temperature increase. The experimental determined flow curves are depicted in Fig. 1.

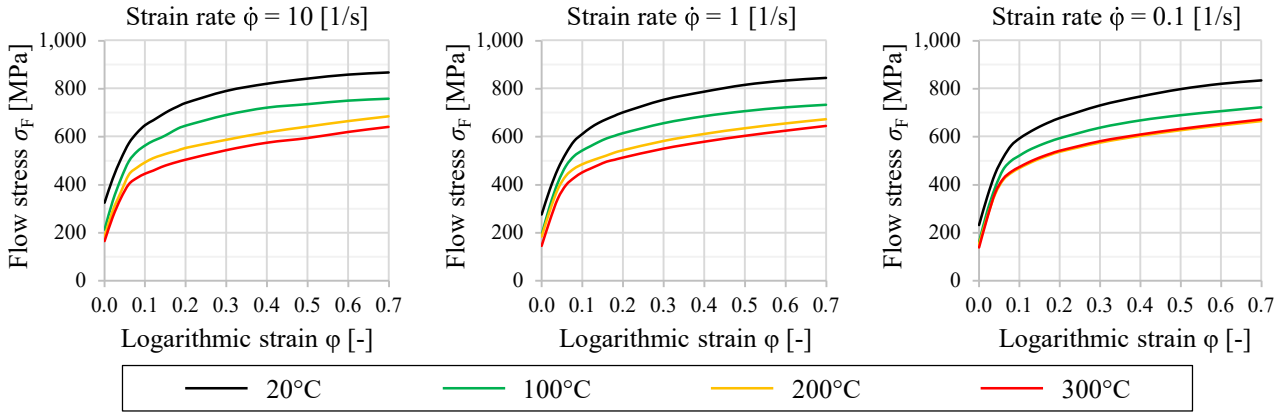

Fig. 1 Experimental determined flow curves for the test material AISI 5115 (16MnCrS5)

At first, a 3D model of the cold forging process with adjustable deformation zone has been developed in DEFORM 3D. Due to the wide variety of parameters and the rather high calculation time of the 3D simulations, the tools were modelled as rigid objects and the workpiece as an ideal-plastic object. This procedure allows the determination of fundamental influences of the splined mandrel geometry on die filling within reasonable calculation time of each individual simulation. The 3D model was designed as a segmented model, whereas the section angle of the considered segment was chosen with regard to the number of teeth of the splined surface. Initially, a convergence analysis was performed concerning the size of the FEM mesh of the workpiece and the considered angle of the segment (half of a tooth versus full tooth). When choosing a mesh size having 200,000 elements modelling one half of a tooth no major differences were found compared to the other investigated variants within the convergence analysis regarding force-stroke-curve and other process state variables. With this number of elements, the minimum element edge length was 0.09 mm. The number of elements was adjusted in each simulation to keep the minimum element edge length of 0.09 mm constant. For the geometric parameter study, shear friction model was used including an initial friction coefficient of $m = 0.1$. During the numerical study, the friction coefficient has also been varied in a range from $m = 0.05$ to $m = 0.15$. The semi-finished product was a tube with a constant length of 58 mm, a constant inside diameter $d_4 = 20$ mm and a variable outside diameter which was initially set

to d_4 = 30 mm. For the numerical investigations no clearance between workpiece and tool was considered.

Fig. 2a shows the developed 3D model for the numerical investigation of the cold forging process with adjustable deformation zone. The model consists of a rigid die, a mandrel and a hollow punch as well as an ideal-plastic workpiece. Due to the developed tool concept in [7], the hollow punch remains stationary while the die moves downwards steadily during the process at a speed of 10 mm/s. The movement of the mandrel, on the other hand, can be controlled upwards or downwards in relation to the hollow punch (Fig. 2a) and is defined as a function of time with speeds of +/- 10 mm/s. Initially, the mandrel is located in its upper position and, therefore, the free cross section right at the end of deformation zone has an annular shape - the desired shape of the workpiece (Fig. 2b). When the mandrel moves towards its lower position, the free cross section at the end of deformation zone does not change in terms of its outside shape, but the inside shape changes to a splined shape (Fig. 2c). In this example, the spline comprises n = 10 teeth.

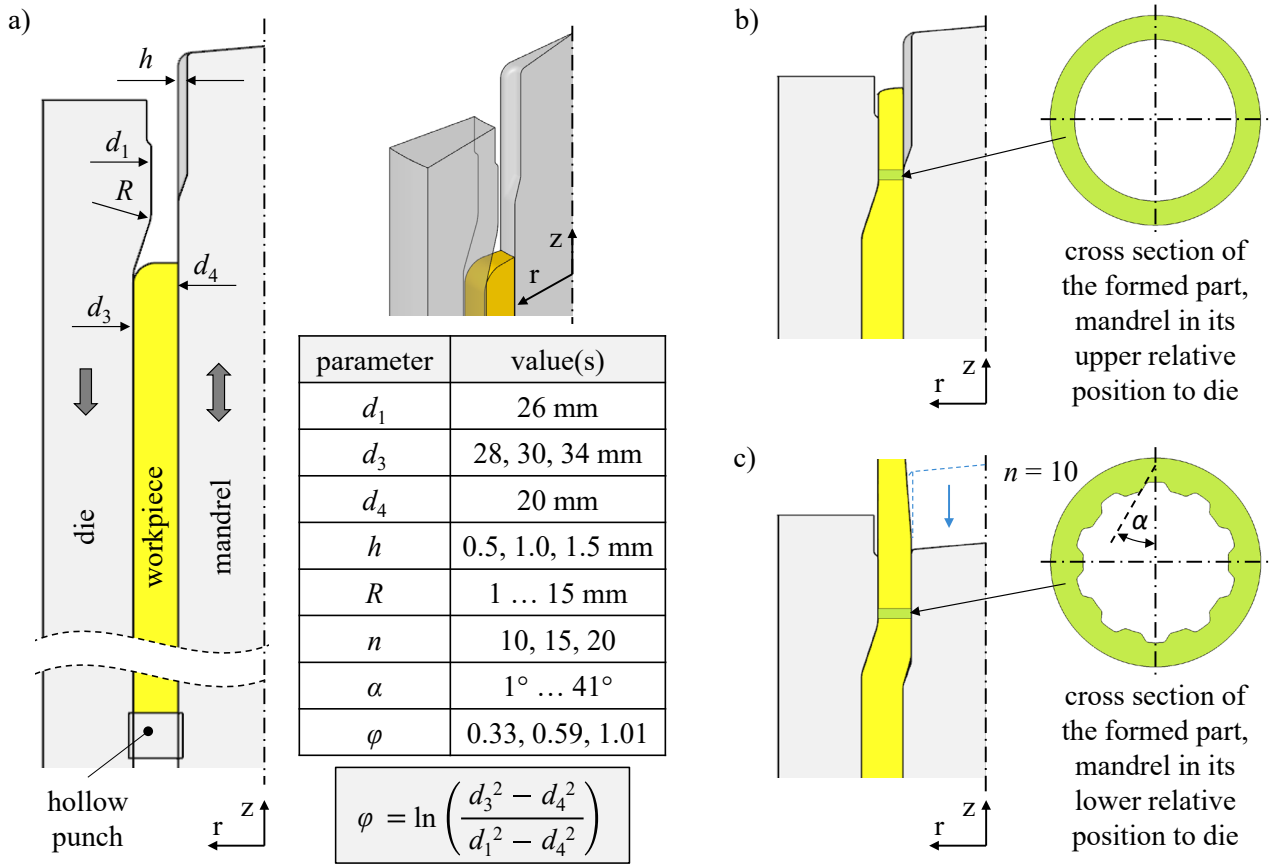

parameter	value(s)
d_1	26 mm
d_3	28, 30, 34 mm
d_4	20 mm
h	0.5, 1.0, 1.5 mm
R	1 … 15 mm
n	10, 15, 20
α	1° … 41°
φ	0.33, 0.59, 1.01

$$\varphi = \ln\left(\frac{d_3^2 - d_4^2}{d_1^2 - d_4^2}\right)$$

Fig. 2: a) Model for numerical investigation, overview of investigated parameters and definition of the logarithmic strain φ according to [9], b) cross section (green) of the formed part with mandrel in its upper position and c) cross section (green) of the formed part with mandrel in its lower position using a splined mandrel with ten teeth

Furthermore, Fig. 2a contains an overview of the used parameters. In this study, spline dependent and independent parameters have been investigated. The tooth height h has been varied between 0.5 mm and 1.5 mm. The number of teeth n has been investigated with 10, 15 and 20 teeth. Also, the tooth flank angle α, which is also shown in Fig. 2c, has been investigated between 1° and 41°. In terms of the spline independent parameters, the radius R at the end of the deformation zone of the die has been varied between 1 mm and 15 mm. Logarithmic strain φ is defined with the formula depicted in Fig. 2a according to [9] and has been investigated by adjusting the diameter d_3. In this case, logarithmic strain φ refers to the cross section change shown in Fig. 2b with the mandrel in its upper position. Nevertheless, also the tooth height h impacts the overall logarithmic strain slightly. In angular sections at the tooth tip of the mandrel, the logarithmic strain corresponds to φ, whereas in

angular sections between two tooth tips of the mandrel, the logarithmic strain is slightly lower. To keep the results more comprehensible, the tooth height h is listed as a separate value instead of a second φ.

For evaluation of the die filling on the outer side of the workpiece, a consistent evaluation methodology has been elaborated, based on a volume comparison. After the forming process of each variant, a characteristic axial section of the pressed part geometry with a length of 30 mm was examined (Fig. 3a). Since the internal splines are not identical for the investigated variants, an angle section comprising half of a tooth was used and the internal splines were cut off in a boolean operation to get the same section in terms of overall length and internal dimension and only the outside shape is specific for each variant (Fig. 3b). Thus, the volume of the sections can be compared to each other, respective to an ideal volume with full die filling and, as a result, the underfilled volume can be determined explicitly. In order to characterize the shape of the internal splines, the spline proportions (run-in length, effective usable length and run-out length) were also determined. In Fig. 3c an exemplary internal spline shape with the characteristic proportions is shown as well as the process states in which these proportions are generated.

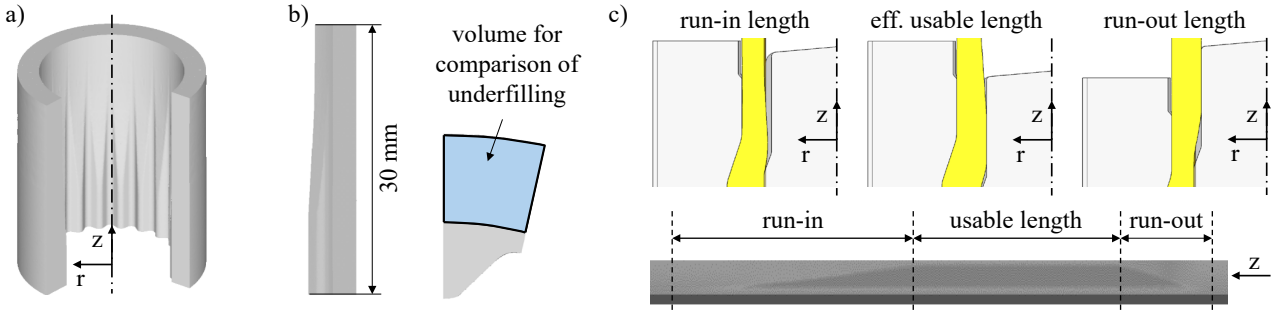

Fig. 3: a) Axial section of the pressed part geometry, b) examined angle section for volume comparison and c) spline proportions (run-in length, effective usable length and run-out length) and process states in which these proportions are generated

At the beginning of the investigations it was determined that the underfilling mainly affects the axial sections of the spline run-in and run-out length. In the remaining sections of the workpiece no underfilling occurs, due to the sufficient back pressure on the mandrel side during these steady process states. The underfilling occurs during the axial movement of the mandrel which leads to a changing deformation zone regarding the free cross section and, thus, to an unsteady process state. By comparing the two possible unsteady process states (change from circular to splined shape and vice versa), it was found that the underfilling emerges significantly higher in the run-in area compared to the run-out area. Therefore, the run-in area was identified as the worst case (largest underfilling volume to be expected) and used for the underfilling analysis.

Results and Discussion

Spline dependent parameters. At first, the spline dependent parameters number of teeth n, tooth height h and tooth flank angle α are evaluated. Fig. 4 depicts the influence of these parameters on volume deviation compared to the ideal volume with no underfilling. The volume deviation decreases with increasing number of teeth from $n = 10$ to $n = 15$, but there is no major change regarding a further increase to $n = 20$ (Fig. 4a). Each tooth tip of the spline of the mandrel represents a radially supporting surface for the plastically deformed workpiece. The more teeth are provided, the closer such radially supporting surfaces are located to each other. With rising tooth height h, the volume deviation at the outside of the workpiece also increases (Fig. 4b). This can be explained by the fraction of volume of the teeth which has to be filled during the cold forging process. Higher teeth in fact do result in a higher volume fraction. This leads to a delayed build-up of back pressure on the mandrel side and, thus, the volume deviation increases. An increasing tooth flank angle from $\alpha = 11°$ to $\alpha = 41°$ tends to lead to an increased volume deviation (Fig. 4c). But there is no clear tendency compared to e.g. number of teeth n or tooth height h since a tooth flank angle $\alpha = 1°$ leads to a similar high volume

deviation as $\alpha = 21$ (Fig. 4c). Thus, there is some kind of a minimum within the investigated values at $\alpha = 11°$.

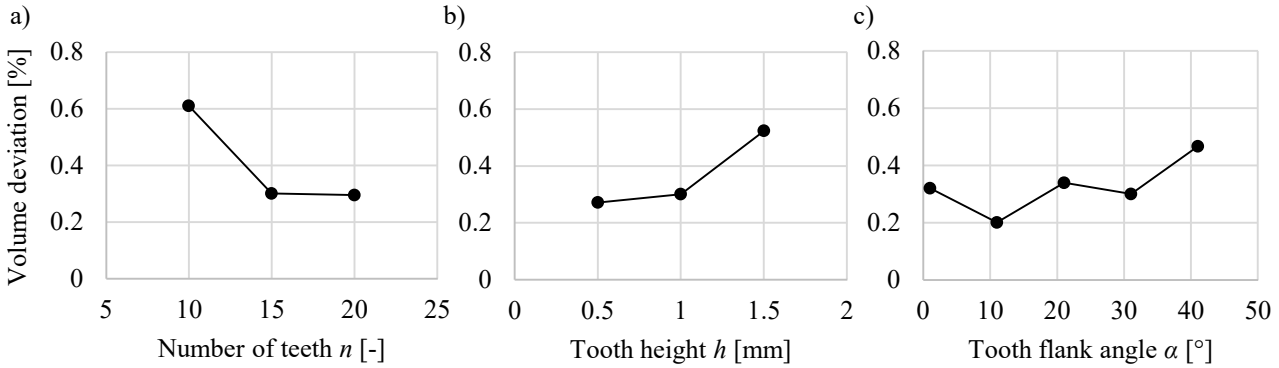

Fig. 4: Influence of spline dependent parameters on volume deviation: a) number of teeth n ($\alpha = 31°$, $h = 1$ mm, $R = 5$ mm, $\varphi = 0.59$), b) tooth height h ($\alpha = 31°$, $n = 15$, $R = 5$ mm, $\varphi = 0.59$) and c) tooth flank angle α ($n = 15$, $h = 1$ mm, $R = 5$ mm, $\varphi = 0.59$)

Fig. 5 shows the influence of the mentioned spline dependent parameters on spline proportions. The already mentioned increased proximity of the radial supporting surfaces of the tooth tips comes with smaller cavities which have to be filled. Despite this improves the volume deviation at the outside of the part, it also leads to an increased run-in length of the spline at the inside of the part. This effect is shown in Fig. 5a. With increasing number of teeth n, run-in length gets larger and, therefore, the effective usable length of the spline gets smaller. The tooth height h has the biggest impact on the spline proportions which can by explained by the increased volume fraction with increasing tooth height and, thus, delayed complete fill of the spline cavities on the mandrel side. Raising the tooth height from $h = 0.5$ mm to $h = 1.5$ mm leads to a significant reduction of the effective usable spline length from 62 % to 12 % (Fig. 5b). The tooth flank angle α shows a similar impact on the spline proportions as the number of teeth (Fig. 5c). With increasing tooth flank angle also the effective usable spline length is reduced.

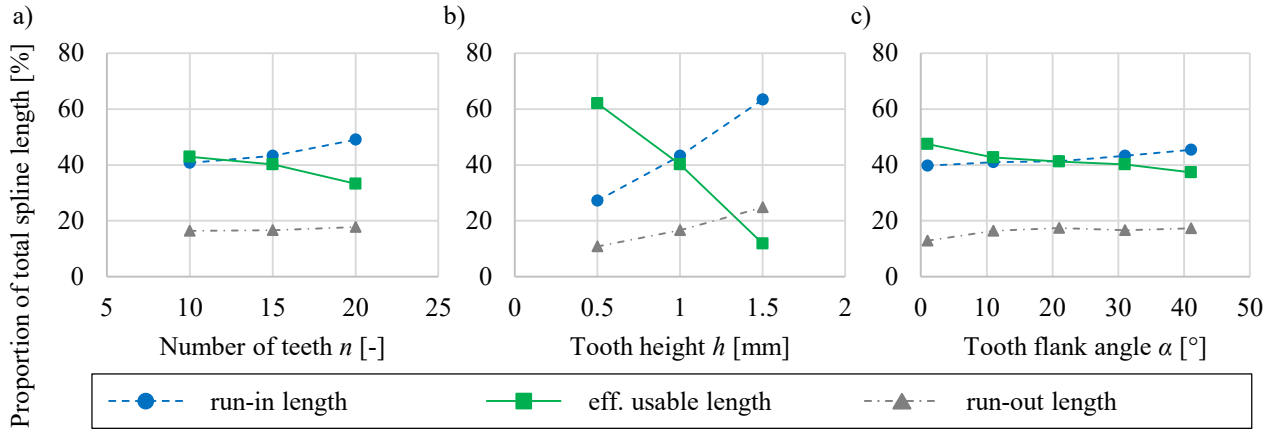

Fig. 5: Influence of spline dependent parameters on spline proportions: a) number of teeth ($\alpha = 31°$, $h = 1$ mm, $R = 5$ mm, $\varphi = 0.59$), b) tooth height ($\alpha = 31°$, $n = 15$, $R = 5$ mm, $\varphi = 0.59$) and c) tooth flank angle ($n = 15$, $h = 1$ mm, $R = 5$ mm, $\varphi = 0.59$)

A detailed look at these results showed that the investigated parameters α, n, R and h all have an impact on the tooth space width (the tangential space between two tooth tips at the constant tooth tip diameter). The tooth space width is measured between the beginning of the radius at the transition from tooth tip to tooth flank at the mandrel (Fig. 6a). In Fig. 6b, the correlation between the tooth space width and the volume deviation is presented. With increasing tooth space width, also the volume deviation increases. This correlation is also shown with the trend line in Fig. 6b. Therefore, the tooth space width is a dominant factor in the formation of underfillings at the outside of the workpiece, whereby an increase in tooth space width in particular has a detrimental effect. For example,

large tooth space widths require an increased specific volume, which leads to a delayed mandrel-side back pressure and favors the formation of underfillings.

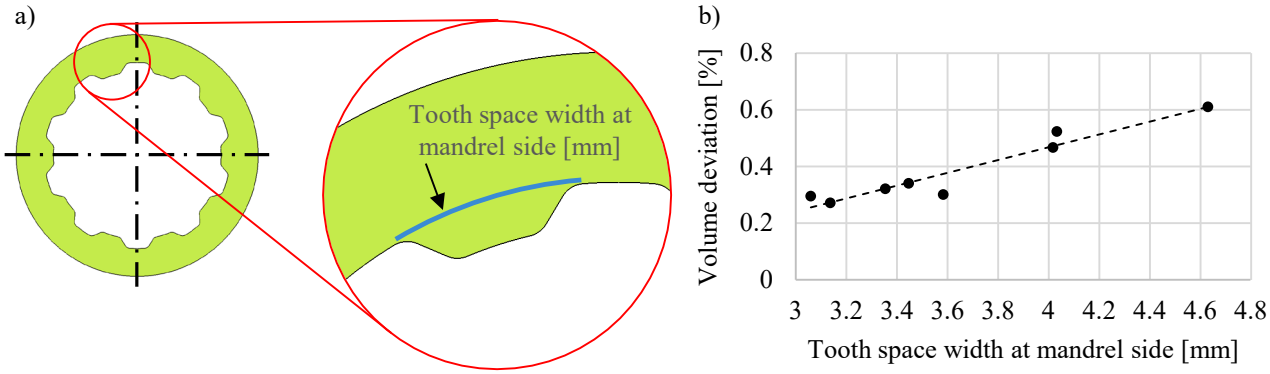

Fig. 6: a) Tooth space width at mandrel side and b) influence of tooth space width at mandrel side on volume deviation

Spline independent parameters. The investigated spline independent parameters radius R and logarithmic strain φ also affect the underfilling at the outside of the workpiece. Among these two parameters, the radius R at the end of the deformation zone of the die has in fact the highest impact on the underfilling phenomenon. In Fig. 7, the radial deviation of the pressed part geometry compared to the ideal outside shape of the workpiece for different radii is presented. Comparatively large radii lead to a significant reduction in underfilling. In contrast, small radii cause a separation of the workpiece material from the inner die surface, resulting in a significantly higher underfill formation. The resulting influence of the radius R on the volume deviation is depicted in Fig. 8a.

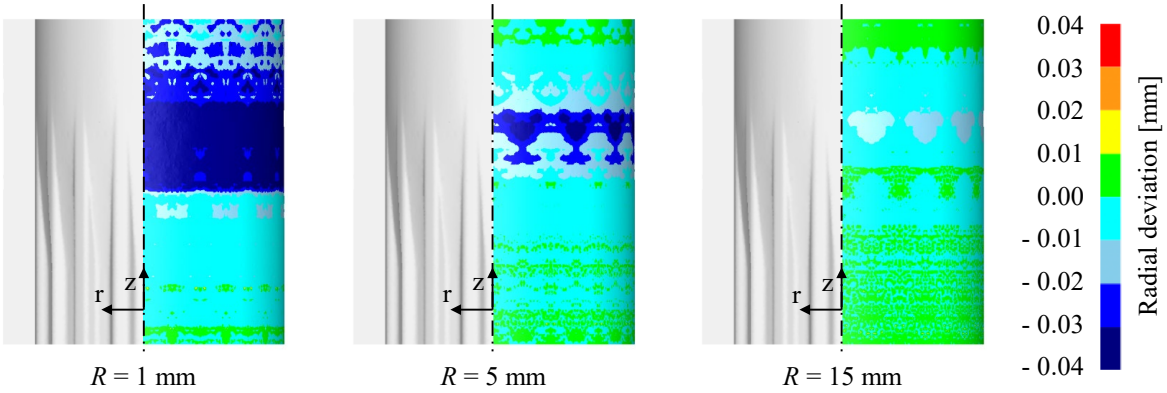

Fig. 7: Radial deviation at the outside of the formed workpiece in the axial section of the run-in length of the internal spline compared to the ideal outside shape for different radii (α = 21°, n = 15, h = 1 mm, φ = 0.59)

In Fig. 8b, the influence of three different logarithmic strain values (φ = 0.33, φ = 0.59, φ = 1.01) for three different tooth heights (h = 0.5 mm, h = 1.0 mm, h = 1.5 mm) on the volume deviation is shown. The logarithmic strain refers to the non-splined cold forged section of the workpiece. As already shown in Fig. 4b, an increased tooth height h leads to higher volume deviation at the part outside. By considering different amounts of logarithmic strain values (Fig. 8b), it can be concluded that higher logarithmic strain values also lead to higher volume deviation. This can be explained by the higher axial velocity of the material flow due to the larger logarithmic strain. Since the axial velocity rises while the radial velocity near the surface of the mandrel does not change significantly, the full filling of the cavity is delayed and, therefore, the underfilling is larger. Regarding the investigated friction values, no major influence of friction values on the underfilling behavior could be determined in general.

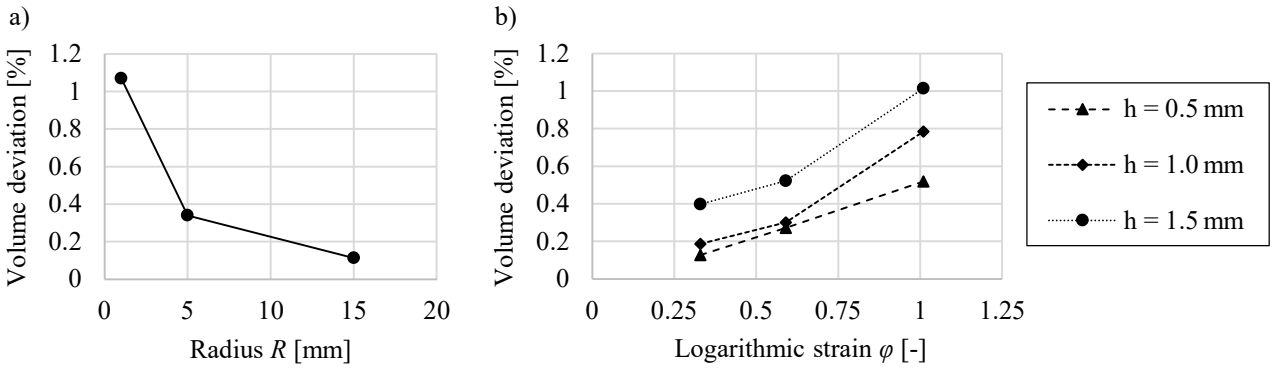

Fig. 8: Influence of spline independent parameters on volume deviation: a) radius on the die side ($\alpha = 21°$, $n = 15$, $h = 1$ mm, $\varphi = 0.59$) and b) logarithmic strain φ of non-splined section in dependence of varying tooth height h ($\alpha = 31°$, $n = 15$, $R = 5$ mm)

During the numerical investigation, also the mandrel kinematic has been adjusted. In Fig. 9a, two different mandrel kinematics are shown in a velocity-time-graph. For this specific investigation, the parameters have been modified slightly to match a real part geometry of a drive shaft ($d_1 = 25.00$ mm, $d_3 = 33.00$ mm, $d_4 = 20.50$ mm, $h = 0.60$ mm, $R = 10$ mm, $n = 24$, $\alpha = 23.25°$). The movement of the die was kept constant with a velocity of 10 mm/s. Kinematic 1 starts with a constant velocity of 10 mm/s and, therefore, at first moves synchronously with the die. Since in this particular investigation the initial position of the mandrel corresponds to Fig. 2c, the internal spline is formed right at the beginning of the process. Afterwards, the velocity is reduced down to 0 mm/s and the deformation zone changes from the splined cross section to the annular one and, thus, the run-out of the spline is formed (Fig. 9b). After this, the mandrel accelerates to 10 mm/s again and moves along the die until the end of the process. In contrast to this simple kinematic, also more complex kinematics have been investigated – for example kinematic 2, which is also depicted in Fig. 9a. With this particular kinematic profile, the mandrel temporarily moves in the opposite direction compared to the die when the deformation zone is changed, which significantly reduces the run-out length (Fig. 9c).

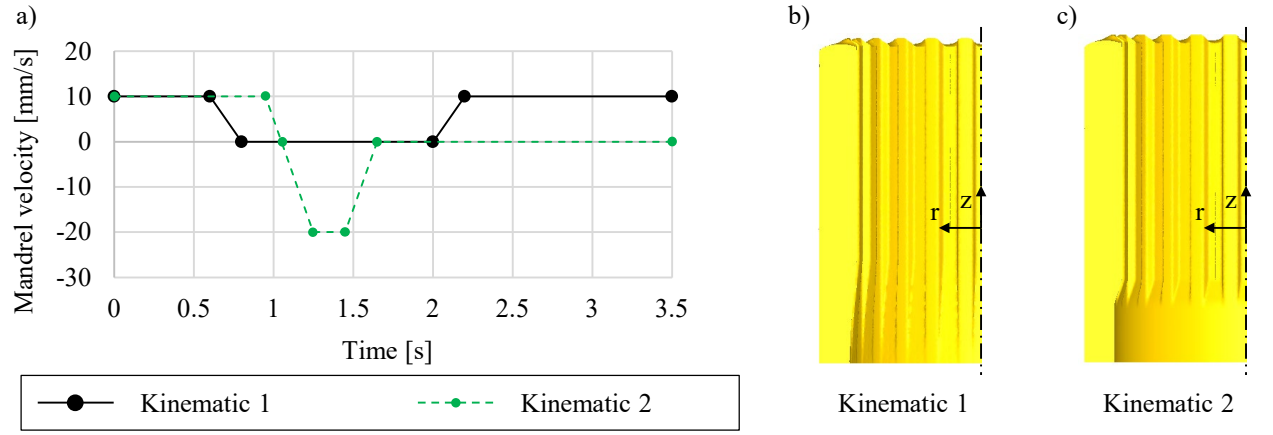

Fig. 9: a) Comparison of two different mandrel kinematics, b) resulting shape of the workpiece using kinematic 1 and c) resulting shape of the workpiece using kinematic 2 ($d_1 = 25.00$ mm, $d_3 = 33.00$ mm, $d_4 = 20.50$ mm, $h = 0.60$ mm, $R = 10$ mm, $n = 24$, $\alpha = 23.25°$)

Conclusion and Outlook

In this contribution, a numerical study on impact of a splined mandrel geometry on die filling in a cold forging process with adjustable deformation zone has been conducted. In particular, spline dependent and independent parameters have been investigated. Regarding spline dependent parameters (number of teeth n, tooth height h and tooth flank angle α), it was found that parameter values that lead to an increasing tooth space width or tooth volume show a negative effect on the filling behavior.

In contrast, such parameter values lead to an increased effective usable spline length at the inside of the workpiece. In terms of spline independent parameters, the radius at the end of the deformation zone of the die has the biggest impact on the underfilling behavior among the investigated parameters. Here, small radii should be avoided for this kind of process. In addition, it was found that larger logarithmic strain values also lead to an increased volume deviation. By adjusting the mandrel kinematic regarding its relative position to the die, it is possible to reduce the run-out length of the internal spline significantly. For the investigated geometry and a desired tooth height of $h = 1$ mm the following parameters should be used as a compromise to keep the outside volume deviation small and simultaneously provide a high effective usable spline proportion at the inside: $\alpha = 11°$, $n = 15$ or higher, $R = 15$ mm and $\varphi = 0.33$. Overall, only very small volume deviations were found in all numerical investigations, indicating the suitability of the process for the production of precise tailored shafts with internal splines.

However, the numerical results must be validated in a next step by means of an experimental investigation. For this purpose, a tool is being manufactured that fulfills the special requirements regarding the investigated tool kinematics. Afterwards, the tool will be installed in a hydraulic press at the Institute for Metal Forming Technology at the University of Stuttgart and experimental investigations will be conducted next. Subsequently, the geometric dimensions of the pressed components will be measured and compared to the numerical results.

Acknowledgments

The research project “Development of a cold forging process for manufacturing hollow parts with variable wall thicknesses” (fund number ZF4012808LP9) in cooperation with LS-Mechanik GmbH is funded by the Federal Ministry of Economic Affairs and Energy through the German Federation of Industrial Research Associations (AiF) as part of the Central Innovation Programme for SMEs (ZIM) based on a decision of the German Bundestag. The authors would like to thank the German Federation of Industrial Research Associations for the financial support. Furthermore, the authors would like to thank the project partner LS-Mechanik GmbH for the collaboration.

References

[1] Liewald, M., Felde, A., Weiss, A., Deliktas, T., 2019, Hollow shafts in lightweight design - state of the art and perspectives, 34. Jahrestreffen der Kaltmassivumformer, VDI.

[2] Hung, N. B., Lim, O., 2020, A review of history, development, design and research of electric bicycles, Applied Energy, 260:18, DOI:10.1016/j.apenergy.2019.114323.

[3] Weiß, A., Liewald, M., 2019, Numerical investigation of a cold forging process for manufacturing hollow shafts with variable wall thickness, NUMIFORM 2019: The 13th International Conference on Numerical Methods in Industrial Forming Processes.

[4] Riley, A., 2012, Plastics manufacturing processes for packaging materials - Blow moulding, in *Packaging technology - Fundamentals, materials and processes*, A. Emblem and H. Emblem, Eds., Woodhead Publishing Limited, 350–359.

[5] Negendank, M., Müller, S., 2018, Strangpressen von Aluminiumhohlprofilen mit axial variabler Wandstärke, 10. Ranshofener Leichtmetalltage - Hochleistungsmetalle und Prozesse für den Leichtbau der Zukunft.

[6] Selvaggio, A., Haase, M., Khalifa, N. Ben, Tekkaya, A. E., 2014, Extrusion of Profiles with Variable Wall Thickness, Procedia CIRP, 18:15–20, DOI:10.1016/j.procir.2014.06.100.

[7] Weiß, A., Liewald, M., 2021, Flexible Fertigung maßgeschneiderter Hohlwellen - Werkzeug und simulative Untersuchung zur Fertigung von Hohlwellen mit Wanddickenvariation, wt Werkstattstechnik online, 111/10:704–708, DOI:10.37544/1436–4980–2021–10–50.

[8] Boutenel, F., Delhomme, M., Velay, V., Boman, R., 2018, Finite element modelling of cold drawing for high-precision tubes, Comptes Rendus Mécanique, 346/8:665–677, DOI:10.1016/j.crme.2018.06.005.

[9] Lange, K., Kammerer, M., Pöhlandt, K., Schöck, J., 2008, Fließpressen - Wirtschaftliche Fertigung metallischer Präzisionswerkstücke, Springer-Verlag Berlin Heidelberg, ISBN: 9783540309093.